Ninth International Conference on CFD in the Minerals and Process Industries
CSIRO, Melbourne, Australia
10-12 December 2012

BEYOND HAMILTONIAN: CHAOTIC ADVECTION IN A THREE-DIMENSIONAL VOLUME PRESERVING FLOW

Daniel R. LESTER[1*], **Lachlan D. SMITH**[2], **Guy METCALFE**[3] **and Murray RUDMAN**[2]

[1]CSIRO Mathematics Informatics and Statistics, Graham Rd, Highett, Victoria 3190, AUSTRALIA

[2]Department of Mechanical Engineering, Monash University, Clayton, Victoria 3800, AUSTRALIA

[3]CSIRO Materials Science and Engineering, Graham Rd, Highett, Victoria 3190, AUSTRALIA

*Corresponding author, E-mail address: daniel.lester@csiro.au

ABSTRACT

The notion that smooth, regular flows can generate complex flow trajectories via *chaotic advection* has widespread implications for fluid transport. Due to the analogy with Hamiltonian dynamics, almost everything is known regarding chaotic advection in 2D flow. Conversely, much less is known regarding 3D flow, chiefly due to breakdown of the Hamiltonian analogy and the explosion of possible Lagrangian topologies. The bestiary of 3D dynamics is only beginning to be uncovered, and a quantitative framework is yet to be fully developed. Furthermore, volume-preserving particle tracking methods in 3D which preserve the conservative nature of the dynamical system are less well-developed than their counterparts for 2D flow. We study chaotic advection in a 3D potential flow, and develop a highly efficient 3D volume-preserving method for the advection equation. The Lagrangian topology of this flow is elucidated, and mechanisms governing global transport identified.

INTRODUCTION

Fluid transport plays a central role in the natural and applied sciences, from oceanic plankton dynamics in geophysical flows to biochemical reactions in microfluidic devices. Although the majority of fluid-borne processes involve additional phenomena such as diffusion, inertia, or chemical reaction, the underlying *passive* transport plays a critical role in organizing material distributions which can profoundly influence the overall dynamics of the coupled system [9]. As such, it is instructive to consider the dynamics of passive transport as quantified by the advection equation

$$\dot{\mathbf{x}} = \mathbf{v}(\mathbf{x},t), \tag{1}$$

describing the evolution with time t of the spatial position $\mathbf{x}$ of a fluid particle under the action of the fluid velocity field $\mathbf{v}(\mathbf{x},t)$. The consideration of (1) from a dynamical systems perspective has generated significant and novel insights into transport and mixing [14], specifically the notion that (1) is a nonlinear dynamical system capable of exhibiting chaotic dynamics for flows with a minimum of three degrees of freedom (e.g. 2D transient or 3D steady flow). If the flow is incompressible, $\nabla \cdot \mathbf{v} = 0$, then the dynamical system (1) is conservative, with physical space $\mathbf{x}$ forming the state space of the system.

In terms of fluid transport, a key consideration is whether the flow $\mathbf{v}$ is mixing, or more formally whether a fluid particle trajectory is globally *ergodic*, in that with time the trajectory visits every point within a closed flow domain. Turbulent flows exhibit ergodicity and rapid mixing, as evidenced by the rate of turbulent dispersion in the presence of diffusion. In general, if (1) exhibits chaotic dynamics, then the flow is a mixing flow over some region of the Lagrangian topology. As such behaviour is kinematic in origin, chaotic dynamics is possible in flows which are smooth and regular (i.e. non-turbulent) in the Eulerian frame. This phenomena, termed *chaotic advection* or *Lagrangian chaos* has elucidated the mechanisms by which low Reynolds number flows can achieve rapid, complete mixing which is highly energy efficient and imparts minimal shear.

In the case of two-dimensional (2D) incompressible flows, the advection equation (1) takes the form of a 1 degree-of-freedom Hamiltonian system, where the streamfunction Ψ plays the role of the Hamiltonian. As such, the theoretical framework, tools and techniques of Hamiltonian mechanics can be directly applied to study transport in 2D flows, where the main results of Hamiltonian chaos directly inform chaotic advection. Consequently, chaotic advection in 2D is very well understood, which has led to a wide variety of insights and applications regarding e.g. geophysical flows, microfluidics, and industrial mixing.

Conversely, much less is known about Lagrangian chaos in three-dimensional (3D) flows; this disparity of understanding is due to a variety of factors [18]. First, the extra spatial dimension admits a much richer array of topological structures and attendant dynamics. The set of topological complexity and associated bifurcation structures are only beginning to be unpicked, and there is much that is unknown regarding routes to chaos in 3D systems. Second, although 3D steady systems can be transformed into 2D unsteady Hamiltonian systems, this Hamiltonian analogy breaks down at stagnation points of the 3D flow. These points play an important role in the generation of chaotic dynamics in 3D systems [1]. Thirdly, although the Kolmogorov–Arnold–Moser (KAM) theorem which plays a key role in describing the fate of invariant tori in 2D systems does have a counterpart in 3D flows [3], this theory is not yet fully developed.

In general, the theory behind 3D systems is less well-developed [18], highlighting the need for fundamental research into 3D systems both in terms of theoretical framework and the dynamics of specific systems. Although this gap is being bridged by recent works, there are many unanswered questions regarding the nature of chaotic advection and transport in 3D flows, representing a rich field of scientific enquiry.

Whilst the study of chaotic advection in 3D inviscid flows, Stokes and laminar flows has received significant attention, no studies have considered chaotic advection in 3D potential flows, and only a handful consider 2D potential flows [10, 11]. There exist a wide range of porous media applications (e.g. geothermal energy [8], carbon sequestration, groundwater transport [17]) in which chaotic advection in 3D potential flows plays a pivotal role, and so understanding the mechanisms of chaotic advection in these systems represents a problem of considerable interest.

As steady potential flows are irrotational, closed fluid orbits are prohibited and so homoclinic/heteroclinic connections (which are considered the "fingerprint of chaos") between stable and

unstable manifolds cannot form. Similarly, although Darcy flows admit non-zero vorticity $\omega \equiv \nabla \times \mathbf{v}$ via the inhomogeneous permeability field, the local helicity $h \equiv \omega \cdot \mathbf{v}$ of the flow (a measure of spatial complexity) is identically zero. Sposito [16] shows that under this identity, Darcy flow streamlines are confined to non-intersecting Lamb surfaces which are topologically flat 2D manifolds. By the Poincaré-Bendixson theorem, continuous systems require a minimum of 3 degrees of freedom to exhibit chaotic dynamics, and so *steady* potential and Darcy flows do not produce Lagrangian chaos. Hence time-dependent flow is a necessary condition for chaotic advection in potential and Darcy flow.

In this paper we study chaotic advection in a transient 3D potential flow in order to identify mechanisms controlling transport in such flows. We consider a dipole flow constrained to the unit sphere Ω, where transient flow may be invoked by transient forcing of the dipole. The simplest transient flow protocol involves punctuated reorientation of the dipole at integer multiples of dimensionless time τ by a fixed angle Θ, and so the transient flow is termed a 3D reoriented potential mixing (3D RPM) flow. This reorientation protocol is closely related to the corresponding 2D analogue [7], which exhibits global chaos for certain flow parameter values τ, Θ.

The Lagrangian dynamics of the 3D RPM flow is studied via both theoretical analysis and numerical integration of the advection equation (1), where particle tracking forms the kernel of a range of tools to investigate the Lagrangian topology and attendant dynamics, coherent structures, periodic points and associated invariant manifolds. As such, it is necessary to use explicitly volume-preserving numerical integrators. Such methods strictly preserve the conservative structure of (1), and eliminate spurious particle attractors and repellers over arbitrarily long integration times.

The development of 3D volume-preserving (VP) numerical integrators is significantly less advanced than that for 2D, where 2D methods draw upon the wide class of symplectic integration methods, which is not possible in 3D. We consider appropriate 3D VP integrators for the 3D RPM flow, and develop a highly efficient VP numerical method based upon a numerical map generated by *a priori* integration of (1). Numerical experiments suggest this method is around 5,000 times faster than direct numerical integration, and this method is used to identify the Lagrangian topology of the flow and the mechanisms governing global transport.

FLOW GEOMETRY AND DYNAMICS

Steady Three-Dimensional Dipole Flow

In this study we consider a 3D RPM flow similar to the 2D transient potential flow considered by Lester et al [7]. This transient flow is composed from a steady 3D dipole flow $\tilde{\mathbf{v}}$ constrained within the unit sphere Ω and driven by a singular source/sink at $(x,y,z) = (0,0,\pm 1)$. As $\tilde{\mathbf{v}} = \nabla\Phi$ is axisymmetric about the z-axis, the cylindrical coordinates (ρ,ϕ,z) form a natural coordinate system to describe the flow, and the flow potential Φ is governed by

$$\nabla^2\Phi = 0, \text{ and } \mathbf{n}\cdot\nabla\Phi\big|_{\partial\Omega} = \delta(z-1) - \delta(z+1), \qquad (2)$$

where $\mathbf{n}$ is the outward unit vector normal to the spherical boundary $\partial\Omega$, and δ is the Dirac delta function. As such, the flow normal to the spherical boundary is zero everywhere except for the singularities at $z = \pm 1$, and the tangential flow is defined by a stress-free (slip) boundary condition. To solve the potential flow we use the method of images [4] for the Neumann

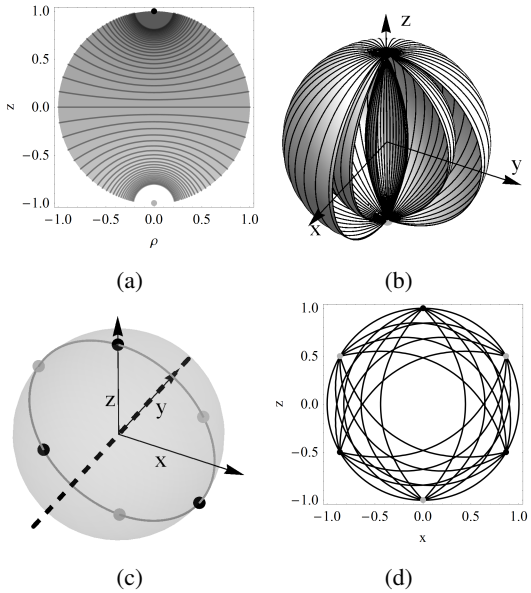

Figure 1: (a) Contours of the axisymmetric potential function Φ. (b) Level surfaces of the axisymmetric stream function Ψ. (c) Reorientation protocol for $\Theta = 2\pi/3$. (d) Superposed streamfunction contours under rotation $\Theta = 2\pi/3$.

boundary problem (2), which yields an analytic solution for Φ,

$$\Phi(\rho,z) = \frac{1}{2\pi}\left(\frac{1}{\sqrt{\rho^2+(1+z)^2}} - \frac{1}{\sqrt{\rho^2+(1-z-)^2}}\right) + \frac{1}{4\pi}\log\left(\frac{1-z+\sqrt{\rho^2+(1-z)^2}}{1+z+\sqrt{\rho^2+(1+z)^2}}\right), \qquad (3)$$

the contours of which are illustrated in Figure 1a. The steady flow $\tilde{\mathbf{v}}$ may also be described in terms of the axisymmetric Stokes streamfunction Ψ,

$$\Psi(\rho,z) = \frac{1-z^2-\rho^2}{4\pi}\left(\frac{1}{\sqrt{(1-z)^2+\rho^2}} + \frac{1}{\sqrt{(1+z)^2+\rho^2}}\right), \qquad (4)$$

where $\tilde{\mathbf{v}} = \nabla\times(\Psi/\rho)\hat{\mathbf{e}}_\phi$. To close the flow domain Ω, we impose periodic boundary conditions at $z = \pm 1$, under the constraint that fluid particles which exit at the sink $z = -1$ are instantaneously re-injected at the source $z = 1$, with the streamfunction Ψ and azimuthal angle ϕ are preserved upon re-injection. Although this re-injection protocol is somewhat artificial, it generates the clearest exposition of the Lagrangian dynamics, which form a basis for consideration of more complex re-injection protocols.

Hence fluid streamlines reside on stream-surfaces of constant Ψ, which in conjunction with the azimuthal angle ϕ form a pair of invariants of the steady flow $\tilde{\mathbf{v}}$, i.e. $\nabla G\cdot\tilde{\mathbf{v}} = 0$ for $G = \Psi,\phi$. As such, streamlines of $\tilde{\mathbf{v}}$ are given by the orthogonal intersections ($\nabla\Psi\cdot\nabla\phi = 0$) of level surfaces of Ψ with level surfaces of ϕ, as illustrated in Figure 1b. Although the confinement of streamlines to invariant surfaces is trivial for the steady flow $\tilde{\mathbf{v}}$, these concepts also extend to the control of transport in the Lagrangian frame for transient flows.

The *flow* (in the dynamical systems sense) of (1) for $\mathbf{v} = \tilde{\mathbf{v}}$ is denoted $\tilde{\Upsilon}_t$, where $\tilde{\Upsilon}_0(\mathbf{X}) = \mathbf{X}$, and $\frac{d}{dt}\tilde{\Upsilon}_t(\mathbf{X}) = \tilde{\mathbf{v}}\big(\tilde{\Upsilon}_t(\mathbf{X})\big)$, where $\mathbf{X}$ are the Lagrangian coordinates. Symmetries of the flow $\tilde{\Upsilon}_t$ govern the Lagrangian topology of the 3D RPM flow and impose constraints upon scalar transport. $\tilde{\Upsilon}$ possesses two basic

symmetries: axisymmetry about the z-axis and a reflection reversal symmetry in the xy-plane. Algebraically these can be written respectively as

$$\tilde{\Upsilon}_t = R^z_\theta \tilde{\Upsilon}_t R^z_{-\theta}, \tag{5}$$

$$\tilde{\Upsilon}_t = S_{xy} \tilde{\Upsilon}_t^{-1} S_{xy}^{-1}, \tag{6}$$

respectively, where R^ξ_θ denotes rotation through angle θ about the ξ-axis and $S_{\xi\zeta}$ denotes reflection in the $\xi\zeta$-plane. The symmetries (5), (6) play an important role in controlling the transport dynamics of the transient flow.

Transient Three-Dimensional Flow

To program the transient 3D RPM flow from the steady flow $\tilde{\mathbf{v}}$, we consider a reorientation protocol which involves reorientation of $\tilde{\mathbf{v}}$ by fixed angle Θ through the xz equatorial plane normal to the y-axis, as per Fig. 1c. The instantaneous reorientation occurs at integer multiples of fixed dimensionless time $t' = \tau$, where dimensionless time $t' = t/t_c$ and t_c is the emptying time t_c of Ω under the steady flow $\tilde{\mathbf{v}}$ (henceforth primes are dropped). The transient flow is given by the piecewise steady approximation

$$\tilde{\mathbf{v}}(\mathbf{x},t) \approx \tilde{\mathbf{v}}\left(R^y_{\lfloor \frac{t}{\tau} \rfloor \Theta}\mathbf{x}, t\right), \tag{7}$$

where the floor function $\lfloor x \rfloor$ denotes the integer part of x. The approximation is made in (7) that the internal flow field within Ω reorients instantaneously, which is justified in cases where the Strouhal number $St = Re/\tau$ is small. As the Reynolds number Re for flow within porous media is negligible, the piecewise steady velocity approximation (7) is valid everywhere except in singular limit $\tau \to 0$.

VOLUME PRESERVING METHODS FOR THE ADVECTION EQUATION

3D Volume Preserving Integration

The study of fluid transport in incompressible flow relates to the propagation of (1) under the constraint $\nabla \cdot \mathbf{v} = 0$, where numerical methods to solve (1) form the kernel of a range of tools and techniques to understand and visualize transport. As the incompressibility constraint renders this dynamical system conservative, such methods must explicitly enforce this constraint over extremely long time-periods, to avoid spurious artifacts such as particle repellers and attractors. Hence whilst numerical solution of (1) shall involve some level of approximation of the governing set of ODEs, the VP constraint must be enforced exactly.

The volume-preserving nature of (1) for incompressible flow means that the fluid deformation tensor

$$\mathbf{F} = \int_{\mathbf{X}} \nabla \mathbf{v}(\mathbf{X},t) dt, \tag{8}$$

must satisfy $\det \mathbf{F} = 1$, and so volume-preserving methods must also satisfy this condition in a numerical sense.

For 2D incompressible flow, the advection equation takes the form of a 1 degree-of-freedom Hamiltonian system, where the streamfunction ψ plays the role of the Hamiltonian H. In general, all d degree-of-freedom Hamiltonian systems are *symplectic*, such that the Jacobian matrix J is a $2d \times 2d$ symplectic matrix;

$$J^T M J = M, \tag{9}$$

where M is a nonsingular, skew-symmetric matrix, such as the block matrix

$$M = \begin{pmatrix} 0 & I_d \\ -I_d & 0 \end{pmatrix} \tag{10}$$

with I_d the $d \times d$ identity matrix. Hence for 2D incompressible flow, numerical methods to solve (1) must be both area-preserving and symplectic to preserve the Hamiltonian structure, which corresponds to enforcing fluid particles exactly follow their streamlines and the streamfunction ψ is conserved. The area-preserving and symplectic conditions are one and the same in 2D, and are satisfied if the Jacobian J_N of the numerical method which propagates the particle position $\mathbf{x}$ to $\mathbf{x}'$ must satisfy

$$\det J_N = \det\left(\frac{\partial x_i'}{\partial x_j}\right) = 1, \tag{11}$$

which is equivalent to the condition $\det \mathbf{F} = 1$ for the fluid deformation tensor.

There exist a wide class of numerical methods which can be rendered symplectic, ranging from common integration techniques such as Crank-Nicholson, Runge-Kutta and various adjoint compositional and splitting methods, through to variational integrators and generating function integrators which are inherently symplectic. In general, VP flows are not symplectic if the number of spatial dimensions is odd, and embedding in a higher-dimensional symplectic domain with even dimensions does not strictly ensure the original system is VP. As such, the development of VP methods in 3D and odd-dimensional domains in general represents a distinct field from symplectic integration methods.

The general field of so-called geometric integrators is concerned with the development of methods which preserve an inherent property (i.e. symmetry, energy, measure) of an ODE system, under which VP forms one such example. This approach is employed by Finn and Chacón [5] to n-dimensional VP methods for divergence-free velocity fields given on a discrete grid of points. Explicitly, as the 3D velocity field $\mathbf{v}$ is incompressible, it may be expressed in terms of the velocity potential $\mathbf{v} = \nabla \times \mathbf{A}$, where the potential $\mathbf{A}$ may be decomposed in cartesian coordinates as

$$\nabla \times \mathbf{A} = \nabla A_x \times \hat{\mathbf{e}}_x + \nabla A_y \times \hat{\mathbf{e}}_y + \nabla A_z \times \hat{\mathbf{e}}_z. \tag{12}$$

As such, a VP scheme $N(h)$ to propagate (1) forward by timestep h can be constructed via operator splitting as

$$N(h) = N_x(h) + N_y(h) + N_z(h), \tag{13}$$

where each N_ζ represents a 2D symplectic method, and the scheme may be extended to second-order accuracy via the time-symmetric decomposition

$$N(h) = N_x(h/2) + N_y(h/2) + N_z(h) + N_y(h/2) + N_x(h/2). \tag{14}$$

This method can be applied to discrete divergence-free velocity data given on a tensor product grid to yield a continuous integration method which is explicitly volume-preserving.

Volume-Preserving Integration in Curvilinear Coordinates

To solve the advection equation (1) for the 3D RPM flow (7), we employ this method in the cylindrical coordinates (ρ, θ, z). Finn and Chacón present an extension of their basic method to yield an explicitly VP integration method in arbitrary curvilinear coordinates ξ^i. Here the velocity field is expressed in contravariant form as

$$\mathbf{v} = v^1 \nabla\xi^2 \times \nabla\xi^3 + v^2 \nabla\xi^3 \times \nabla\xi^1 + v^3 \nabla\xi^1 \times \nabla\xi^3, \tag{15}$$

where

$$v^i = J_\xi \mathbf{v} \cdot \xi^i, \tag{16}$$

and J_ξ is the Jacobian of the coordinate transform, $J_\xi = |\det(\partial\xi^i/\partial x^k)|$. In this coordinate system the equations of motion become

$$\frac{d\xi^i}{dt} = \mathbf{v}\cdot\nabla\xi^i = \frac{v^i}{J_\xi}, \tag{17}$$

and so for the vector potential in contravariant components $\mathbf{A} = \sum_i A_i \nabla\xi^i$, the velocity is given as the formal curl of $\mathbf{A}$:

$$\mathbf{v} = \varepsilon^{ijk}\frac{\partial A_k}{\partial\xi^j}. \tag{18}$$

As such, the advection equation in curvilinear coordinates (17) is of the same form as that for cartesian coordinates (1) with the exception of the Jacobian factor $1/J_\xi$. This system may be re-cast in terms of the integration variable λ where

$$\frac{d\xi^i}{d\lambda} = v^i, \quad \frac{dt}{d\lambda} = \frac{1}{J}, \tag{19}$$

such that fluid particles follow the same orbits, and λ represents a locally stretched time coordinate.

VOLUME-PRESERVING INTEGRATION OF THE 3D RPM FLOW

Volume-Preserving Integration of the 3D RPM Flow

For the cylindrical coordinate system, the Jacobian $J_\xi = \rho$, and so for the steady flow $\tilde{\mathbf{v}}$ with zero swirl ($v_\theta = 0$), the set of advection equations including the stretched time coordinate λ are

$$\frac{d\rho}{d\lambda} = \rho\tilde{v}_\rho(\rho,z),\ \frac{d\theta}{d\lambda} = 0,\ \frac{dz}{d\lambda} = \rho\tilde{v}_z(\rho,z),\ \frac{dt}{d\lambda} = \rho. \tag{20}$$

Hence volume-preserving integration of the 3D RPM flow (7) corresponds to symplectic integration of (20) where only one of the numerical integration steps in (13) is required. In general, the method described is capable of explicit volume-preserving integration of steady and unsteady flows in general curvilinear coordinates.

In general, integration of the advection equation for 2D area-preserving flows may be performed analytically via the change of coordinates

$$\tilde{\mathbf{v}}(x_1,x_2) \mapsto \tilde{\mathbf{v}}(\Psi,\zeta), \tag{21}$$

where ζ is a coordinate orthogonal to Ψ. As the streamfunction Ψ is preserved, the 1D advection equation

$$\frac{d\zeta}{dt} = \tilde{\mathbf{v}}(\Psi,\zeta), \tag{22}$$

may be integrated analytically to directly yield an expression for advection time as a function of ζ. Whilst this is possible for the 2D dipole flow [7], the quartic form of the streamfunction Ψ prevents this for the 3D dipole (4), and so numerical methods are required to directly integrate (20).

We consider two symplectic methods for the integration of (20); a fourth-order Gauss-Legendre (GL) method and a fourth-order Runge-Kutta (RK) method across a range of step sizes. The implicit Gauss-Legendre method is solved using Picard iteration to machine precision (10^{-16}). The global error in the streamfunction Ψ from the initial value is order 10^{-15} for 2000 integration steps of size $\tau = 0.1$. The GL method is significantly more accurate than RK, with global errors in Ψ of order machine precision obtained for time steps $\Delta t = 10^{-4}$, which appear to plateau after 1000 iterations. As such, the fourth-order GL method accurately preserves the symplectic structure of (20).

Volume-Preserving Mapping of the 3D RPM Flow

Although the GL method is relatively efficient, the large number of particle trajectories and long integration times involved in study of the Lagrangian topology render particle tracking a significant computational overhead. Although it is not possible to place the advection equation (1) in the 1D form (22), it is possible to numerically solve the equivalent ODE system (20) *a priori* to high resolution throughout the domain Ω to form a volume-preserving numerical map of the flow $\tilde{\Upsilon}_t$.

Due to the underlying symmetries (5), (6) of the steady flow field $\tilde{\mathbf{v}}$, it is only necessary to solve (20) over the quarter disc $\Omega_1 : z \leqslant 0, \rho \geqslant 0$, with $\Psi \in [0,\pi/4]$. To construct the set of numerical solutions to (20), we choose a set of initial conditions $\Psi_i = i\pi/4000$ for $i = 0,1,\ldots,1000$ along the $z = 0$ axis, and the GL method with timestep 10^{-5} is used to integrate the particle trajectories to the sink at $z = -1$. The coordinate system (Ψ,z) is used define the position of a particle, where the integration points for each value of Ψ_i from $z = 0$ to the dipole sink at $z = -1$ are interpolated in z to generate the continuous function $z = Z_{N,i}(\Psi_i,t')$, where the advection time is re-scaled as $t' = t/T(\Psi_i)$, where T_i is total travel time to the dipole sink at $z = -1$, hence $t' \in [0,1]$.

The continuous numerical map $Z_N(\Psi,t)$ over $\Psi \times t' = [0,\pi/4]\times[0,1]$ is then constructed by interpolation over the set of functions $Z_{N,i}(\Psi_i,t')$ in Ψ. Mapping of Z_N via the reflection symmetry (6) expands the domain to $z \in [-1,1]$, $t/T(\Psi) \in [-1,1]$ where negative values of t correspond to positive values of z. Whilst advection via the numerical map Z_N introduces numerical errors via interpolation and integration, Z_N explicitly preserves the streamfunction Ψ and so is symplectic.

To advect fluid particles forward in space, it is also necessary to construct the inverse numerical map $t = T_N(\Psi,z)$ which may be implemented via a Newton-Raphson method for $Z_n(\Psi,t)$ for fixed Ψ. Similarly, this map is symplectic in that T_N contains numerical errors in z but explicitly preserves Ψ. As such, advection of a fluid particle at (z_n,Ψ) under the steady flow $\tilde{\mathbf{v}}$ over time period τ is mapped to (z_{n+1},Ψ), as

$$z_{n+1} = Z_N(t_{n+1},\Psi), \tag{23}$$

$$t_{n+1} = \left(T_N(z_n,\Psi) + t + \frac{T(\Psi)}{2} \mod T(\Psi)\right) + \frac{T(\Psi)}{2}, \tag{24}$$

where the mod operator encodes re-injection of fluid particles whilst preserving Ψ, ϕ.

The 2D symplectic map Z_N forms the basis of a 3D volume-preserving map for the piecewise steady velocity field $\mathbf{v}$ (7), by composition with the reorientation operator R^y_Θ. To simplify visualization, computations are carried out in a frame of reference moving with the 3D dipole, such that the velocity field $\mathbf{v}$ is steady, and fluid particles are reoriented by $R^y_{-\Theta}$ at integer multiples of the reorientation time τ as follows.

If we consider a fluid particle within the 3D domain Ω at position $\mathbf{x}$ described by the coordinate system $\mathbf{x} = (\Psi,\phi,z)$, then the numerical steps (23), (24) form a numerical approximation $\tilde{\Upsilon}_N$ to the map $\tilde{\Upsilon}_\tau$ over one reorientation period which preserves the invariants Ψ, ϕ. Hence propagation of a fluid particle at position $\mathbf{x}_n = \mathbf{x}(n\tau)$ in the dipole frame of reference at integer multiples of τ under $\mathbf{v}$ is given by

$$\mathbf{x}_{n+1} = \Upsilon_N\mathbf{x}_n \equiv R^y_{-\Theta}\tilde{\Upsilon}_{N,\tau}\mathbf{x}_n, \tag{25}$$

As the map Υ_N is based upon the 3D volume-preserving scheme (20) in curvilinear coordinates, this map is also volume-preserving and so may be used to rapidly propagate fluid particles. Numerical experiments suggest the map $\Upsilon_{N,\tau}$ is around

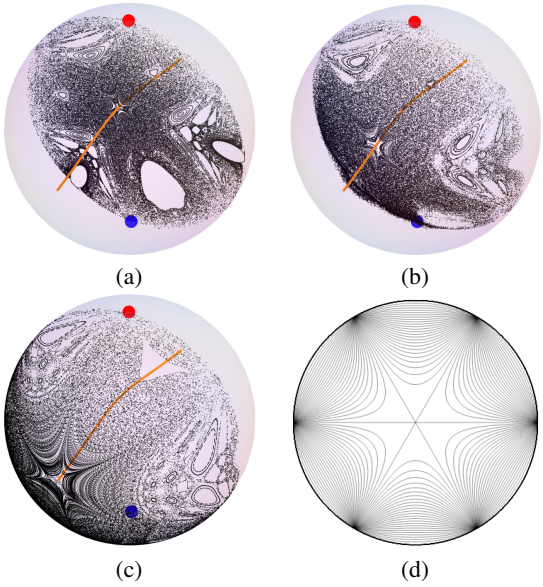

Figure 2: (a)-(c) Nested 2D surfaces within the 3D Poincaré section of the 3D RPM flow for $\Theta = 2\pi/3$ and $\tau = 0.1$, where (a) $G = 0$, (b) $G = 0.5$, (c) $G = 1$. The red/blue dots depicts the dipole source/sink, and the period-1 line is shown in orange. (d) Projection in the xz-plane of the superposed streamfunction Ψ' for $\Theta = 2\pi/3$ in the limit $\tau \to 0$.

5,000 times faster than direct numerical integration of (20) via the symplectic GL method.

LAGRANGIAN TOPOLOGY OF THE 3D RPM FLOW

Poincaré Sections

A first step to understanding chaotic advection and transport in the 3D RPM flow is to elucidate the Lagrangian topology which provides the geometric structure of the advection dynamics. We use the Poincaré map Υ to represent the long-time dynamics of (1) as a 3D object in Ω, termed the Poincaré section, where Υ is given as

$$\Upsilon = R^y_{-\Theta}\tilde{\Upsilon}_\tau. \tag{26}$$

The Poincaré section can be calculated by recording particle positions after each iteration under Υ_N. As the Lagrangian topology is invariant under the counter-rotation $R^y_{-\Theta}$, the dynamics of Υ_N are equivalent to the continuous map in the laboratory frame. By posing the 3D RPM velocity field (7) in the dipole frame, the non-autonomous system (1) is time-periodic over each reorientation period τ, and so (1) may be re-cast as autonomous system with time as an additional state variable [6]. This construction renders the phase space $\Omega \times [0,\tau]$ compact, and so the Poincaré recurrence theorem applies with the Poincaré section taken as the cross section Ω. Toward the limit of many of reorientation periods, the Poincaré map renders a clear representation of the Lagragian topology, where coherent structures corresponding to regular (non-chaotic) regions, which are topologically distinct from ergodic (chaotic) regions of the map. These regions are clearly shown in Fig. 2(a)-(c), which depicts several 2D surfaces of the full 3D Poincaré section for the 3D RPM flow in Ω. The full 3D Lagrangian topology consists of the foliation of these 2D surfaces throughout Ω, which we shall explore in greater detail throughout this Section.

Symmetries of the map Υ

Symmetries play an important role in organising fluid transport, as they impose constraints on both the Lagrangian topology and associated dynamics. The basic symmetries (6), (5) of the steady flow $\tilde{\Upsilon}_t$ impart several symmetries of the stroboscopic map Υ which manifest in the Lagrangian topology. The general axisymmetry (5) contains as a special case the xz reflection symmetry $\tilde{\Upsilon}_t = S_{xz}\tilde{\Upsilon}_t S_{xz}$, and so Poincaré map Υ is symmetric in the xy-plane, where

$$\Upsilon = R^y_\Theta \tilde{\Upsilon}_\tau = R^y_\Theta S_{xz}\tilde{\Upsilon}_\tau S_{xz} = S_{xz}R^y_\Theta \tilde{\Upsilon}_\tau S_{xz} = S_{xz}\Upsilon S_{xz}. \tag{27}$$

As the xz symmetry plane itself is invariant under Υ, without loss of generality we only consider transport in the y^+ hemisphere. Furthermore, the xz-plane acts as an impenetrable barrier which divides Ω into two topologically distinct regions for all τ, Θ.

The other symmetry of Υ is obtained via the reflection reversal symmetry (6) as follows,

$$\Upsilon = R^y_\Theta \tilde{\Upsilon}_\tau = R^y_\Theta S_{xy}\tilde{\Upsilon}_\tau S_{xy} = R^y_\Theta S_{xy}\Upsilon^{-1}R^y_\Theta S_{xy} = S_1\Upsilon^{-1}S_1 \tag{28}$$

where $S_1 = R^y_\Theta S_{xy}$. One can compute that S_1 is the map that reflects a point through the plane $z = \frac{-\sin\Theta}{\cos\Theta+1}x$. Therefore structures in the Lagrangian topology also evolve symmetrically about this plane as, illustrated in Fig. 2(a)-(c) by the reflection symmetry of the coherent structures.

Mode Locking within the 3D RPM Flow

It is instructive to consider the 3D RPM flow $\mathbf{v}$ toward the limit $\tau \to 0$, which corresponds to an steady flow comprising of a superposition of all of the steady flows $\tilde{\mathbf{v}}$ reoriented under R^y_θ. If the reorientation angle Θ is incommensurate with π, then the sequence of dipole positions $\theta = n\Theta$ for $n = 0,1,2,\ldots,\infty$ forms a space-filling set which densely fill the equator. Conversely, if Θ/π is rational such that $\Theta = (j/k)2/\pi$, then the full set of dipole positions form a discrete periodic sequence with period k. As such, the 3D RPM flow for irrational Θ/π in the limit $\tau \to 0$ is identically zero, as the space-filling set of dipole positions result in cancellation of the source and sink terms. Similarly for rational Θ/π with k even, such cancellation occurs and the net flow is zero. Only for the case with Θ/π rational and k odd does the superposed flow remain non-zero for $\tau \to 0$, where the Stokes streamfunction Ψ' of $\mathbf{v}$ is given by the superposition

$$\Psi' = \frac{1}{k}\sum_{i=1}^{k} R^y_{i\Theta}\Psi, \tag{29}$$

where the xz-plane of Ψ' is shown in Fig. 2(d) for $\Theta = 2\pi/3$. As such, for odd k in the limit $\tau \to 0$, the Lagrangian topology is completely regular and k-fold rotationally symmetric (as given by Ψ'). Such *mode locking* persists for small perturbations to finite τ, where the mode-locked region of the parameter space $Q = \tau, \Theta$ widens in Θ with increasing τ, forming Arnol'd tongue-like structures very similar to that observed for the 2D RPM flow [7]. Mode-locked regions for even k also arise at finite τ, and these non-chaotic, mode-locked structures emanate into Q from rational values of Θ/π along the $\tau = 0$ axis.

With increasing τ, these Arnol'd tongues eventually collide and the competing resonances between colliding tongues drive stable elliptic lines to bifurcate to hyperbolic lines via a periodic-doubling cascade around $\tau \sim 1$. This appears to be the primary route to globally chaotic dynamics for the 3D RPM flow. At intermediate values of τ, mixed chaotic and regular dynamics are observed within the Poincaré section, as shown in Fig. 2(a)-(c), where the period-1 elliptic line (shown in orange) and associated coherent structure arising from the k-fold rotationally symmetric streamfunction Ψ' (Fig. 2(d)) can be clearly seen. Other

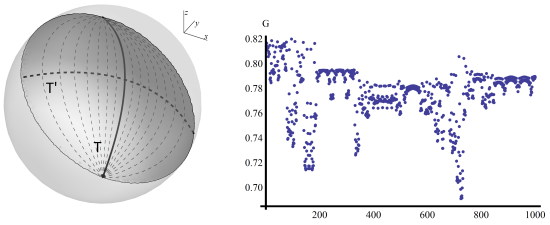

(a) (b)

Figure 3: (a) A level surface of G. The thick solid line is T, the thick dashed line is T', and the dashed lines are streamlines of $\tilde{\Upsilon}_t$ that pass through T'. (b) Perturbations of the invariant G as the particle is advected for 1000 iterations. The scaling is such that $G = 1$ and $G = 0$ correspond to the xz-plane and the spherical boundary respectively.

non-chaotic coherent structures associated with higher-order elliptic lines and associated cantori are also clearly apparent, surrounded by a background chaotic "sea". In 3D these coherent structures form non-chaotic tubes throughout the flow domain Ω, and with increasing τ these structures diminish in size until they are virtually undetectable and the system may be considered to be globally chaotic.

As such, the 3D RPM flow appears to share many qualitative features with its 2D counterpart [7], and so one may consider the 3D system as a foliation of nested 2D surfaces, as indicated by Fig. 2(a)-(c). Of paramount importance is whether fluid transport occurs transverse to these nested 2D surfaces, as this is the mechanism by which complete mixing and ergodic transport within Ω may occur.

Adiabatic Surfaces of the 3D RPM Flow

Detailed analysis shows that fluid particles are not strictly trapped within the 2D shells shown in Fig. 2(a)-(c), but rather hop from shell to shell with time as shown in Fig. 3(a). This behaviour suggests the shells are not invariant under the flow Υ (in which case they would be trapped for all time), but rather the shells form an so-called *adiabatic surfaces* which admit slow transverse transport. In essence, these adiabatic surfaces arise due to the fact that the actions of particle reorientation and advection which comprise Υ admit invariant surfaces which are similar but not the same. If the associated invariant surfaces were identical, this invariant structure would be preserved under the Poincaré map Υ, however small discrepancies between these invariant surfaces allow slow "hopping" as the reorientation and advection operators are iterated. We show this more clearly as follows.

Whilst Ψ, ϕ form an orthogonal pair of invariants of $\tilde{\Upsilon}$, there exist an infinite number of such pairs, and so we may construct another invariant from Ψ, ϕ. Consider the streamline T given by the intersection of $\Psi = \psi_0$ and $\phi = \pi/2$ (see Figure 3(a)). If we rotate this streamline by $\pi/2$ about the y-axis to form T', the surface formed by the union of all streamlines that pass through T' is a level surface of the invariant G, where

$$G(\rho,\theta,z) = \Psi\big(\tilde{\rho}(\Psi(\rho,z))\sin\theta, \tilde{\rho}(\Psi(\rho,z))\cos\theta\big), \quad \text{where } \tilde{\rho}(\psi) = \sqrt{1+2\pi^2\psi^2 - 2\pi\sqrt{2\psi^2+\pi^2\psi^4}}. \tag{30}$$

As G is close to invariant under rotation about the y-axis, the map Υ produces small perturbations in G (as per Fig. 3(b)), and so G forms an adiabatic surface under Υ. The size of these perturbations vary across each adiabatic surface, which decay to zero toward the dipole reorientation equator. As shown in Fig. 3(b), shell hopping for ergodic particles appears to follow a punctuated series of quasi-periodic cycles of varying duration, whilst particles in regular regions follow an indefinite quasiperiodic orbit and so only traverse a fixed number of shells. As such, with time particles in ergodic regions may globally traverse the entire 3D ergodic region, whilst particles in regular elliptic tubes only traverse a fixed region of the tube. Hence when the Lagrangian topology is globally ergodic, fully 3D transport within Ω is possible although limited by transport across adiabatic surfaces. The separation of transport timescales across and within the adiabatic surfaces allow the transport dynamics may be posed in terms of canonical action-angle (slow-fast) variables for which a perturbative framework [12] can be used to quantify the transport dynamics which is a topic of future research.

CONCLUSIONS

We have studied chaotic advection in a 3D transient potential flow, and elucidated the Lagrangian topology over the parameter space $Q = \tau \times \Theta$. A highly efficient mapping method has been developed to solve the advection equation which is explicitly volume-preserving. The Lagrangian topology of the 3D RPM flow is comprised of the foliation of 2D adiabatic surfaces emanating from the xy-plane toward the spherical boundary. The Lagrangian dynamics on these surfaces is qualitatively similar to that of the 2D RPM flow, where regular mode-locked Poincaré sections emanate in Q from rational values of Θ/π along the $\tau = 0$ axis which collide and competing resonances drive a period-doubling route to chaos around $\tau \sim 1$. The nested surfaces in the Poincaré section are adiabatic surfaces which arise from the fact that invariant surfaces under the steady flow $\tilde{\mathbf{v}}$ are close to rotationally symmetric under the transient flow $\mathbf{v}$. The detailed mechanics of adiabatic transport in the 3D RPM flow is yet to be uncovered, but is fundamentally distinct to that observed in other 3D chaotic flows. These results provide the first observations of chaotic advection in a 3D potential flow, which exhibit a wholly new mechanism of 3D transport.

REFERENCES

[1] BAJER, K., (1994), Hamiltonian Formulation of the Equations of Streamlines in three-dimensional Steady Flows, *Chaos Solitons & Fractals*, **4**, 895–911.

[2] CARTWRIGHT, H.E., FEINGOLD, M. and PIRO, O., (1996), Chaotic advection in three-dimensional unsteady incompressible laminar flow, *J. Fluid. Mech.*, **316**, 259–284.

[3] CHENG, C.-G. and SUN, Y.-S., (1990), Existence of invariant tori in three-dimensional measure preserving mappings, *Cel. Mech.*, **47**, 275–292.

[4] DASSIOS, G. and STEN, J.C.-E, (2012), On the Neumann function and the method of images in spherical and ellipsoidal geometry, *Math. Meth. Appl. Sci.*, **35**, 482–496.

[5] FINN, J.M. and CHACÓN, L., (2005), Volume preserving integrators for solenoidal fields on a grid, *Phys. Plasmas*, **12**, 054503.

[6] GUCKENHEIMER, J. and HOLMES, P., (1983), *Nonlinear Oscillations, Dynamical Systems, and Bifurcations of Vector Fields*, Springer-Verlag.

[7] LESTER, D.R. *et al.*, (2009), Lagrangian topology of a periodically reoriented potential flow: Symmetry, optimization and mixing, *Phys. Rev. E*, **80**, 036208.

[8] LESTER, D.R. *et al.*, (2010), Scalar dispersion in a periodically reoriented potential flow: acceleration via Lagrangian chaos, *Phys. Rev. E*, **81**, 046319.

[9] METCALFE, G. *et al.*, (2012), Beyond passive: chaotic transport in stirred fluids, *in Advances in Applied Mechanics, eds van der Giessen, E., Aref, H*, Elsevier.

[10] METCALFE, G. *et al.*, (2012), A partially open porous media flow with chaotic advection: towards a model of coupled fields, *Phil. Trans. Roy. Soc. A*, **368**, 217–230.

[11] METCALFE, G. *et al.*, (2012), An experimental and theoretical study of the mixing characteristics of a periodically reoriented irrotational flow, *Phil. Trans. Roy. Soc. A*, **368**, 2147–2162.

[12] MEZIĆ, I. and WIGGINS, S., (1994), On the integrability and Perturbation of Three-Dimensional Fluid Flows with Symmetry, *J. Nonlinear Sci.*, **4**, 157–194.

[13] MACKAY, R.S., (1994), Transport in 3D Volume-Preserving Flows, *J. Nonlinear Sci.*, **4**, 329–354.

[14] OTTINO, J.M., (1989), *The kinematics of mixing: stretching, chaos, and transport*, Cambridge University Press.

[15] SPEETJENS, M.F.M., CLERCX, H.J.H. and VAN HEIJST, G.J.F., (2006), Merger of coherent structures in time-periodic viscous flows, *Chaos*, **16**, 043104.

[16] SPOSITO, G., (2001), Topological groundwater hydrodynamics, *Adv. Wat. Res.*, **24**, 793–801.

[17] TREFRY, M.G. *et al.*, (2012), Toward enhanced subsurface intervention methods using chaotic advection, *J. Contam. Hydro.*, **27**, 15-29.

[18] WIGGINS, S., (2010), Coherent structures and chaotic advection in three dimensions, *J. Fluid. Mech*, **654**, 1–4.